

ENGINEERING CONSULTING SERVICES

# Assessment of AC Protection Performance in Weakening Systems

## Scottish Hydro Electric Transmission PLC/ The National HVDC Centre

**Attention:** Mr. Bharath Ponnalagan, Dr. Oluwale Daniel Adeuyi  
and Mr. Benjamin Marshall

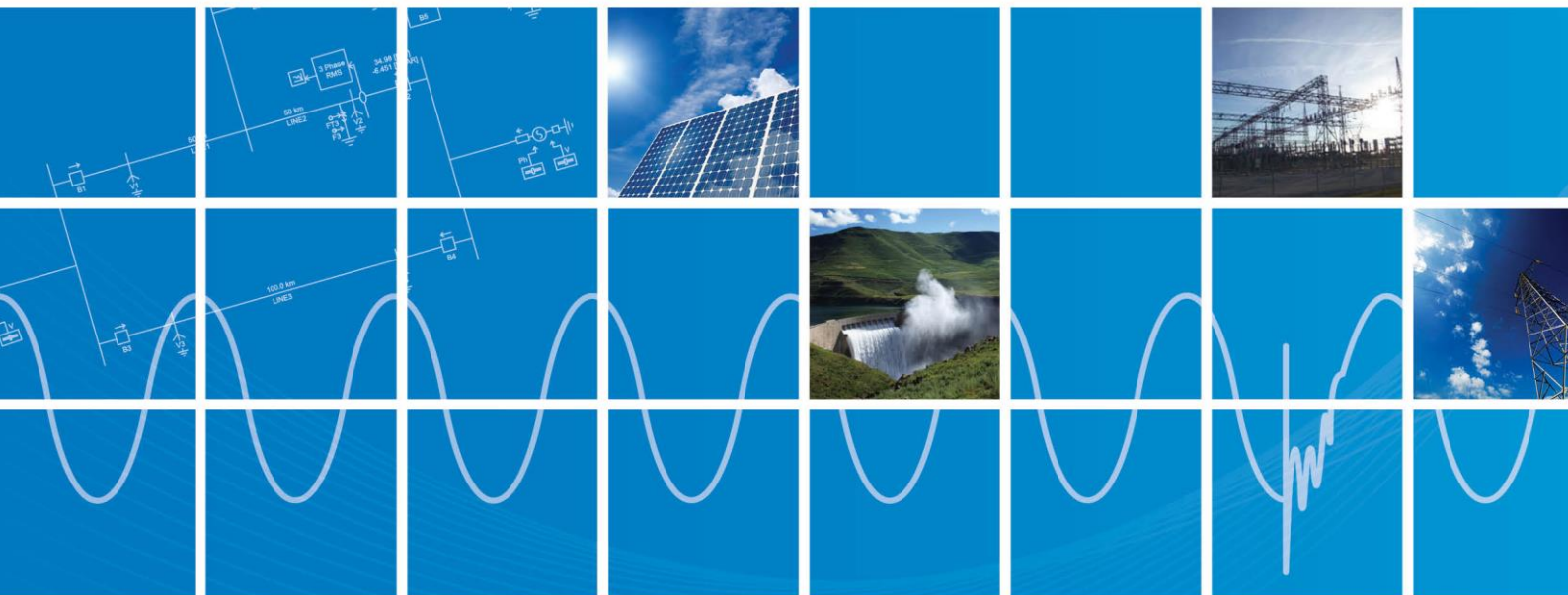
[Bharath.ponnalagan@sse.com](mailto:Bharath.ponnalagan@sse.com)

[oluwale.adeuyi@sse.com](mailto:oluwale.adeuyi@sse.com)

[Benjamin.Marshall@sse.com](mailto:Benjamin.Marshall@sse.com)

+44 (0) 1236 687 248

Date: Aug 13<sup>th</sup>, 2021



## DOCUMENT TRACKING

Rev.	Description	Date
0	First Draft for Initial Comments	May 03 <sup>rd</sup> , 2021
1	Second Draft for Final Comments	July 12 <sup>th</sup> , 2021
2	First Final Issue	August 13 <sup>th</sup> , 2021

## THIRD PARTY DISCLAIMER

Power System Technology Centre (“PTC”), a division of Manitoba Hydro International Ltd. (“MHI”) has prepared this document for the sole use of The National HVDC Centre (“Client”), and for the intended purposes stated in the agreement between MHI and the Client pursuant to which this document was completed.

The content of this document is not intended for the use of, nor is it intended to be relied upon by any person, firm, corporation or other governmental or legal entity (each a “Third Party”), other than the Client. MHI makes no warranty, express or implied, to any Third Party in relation to the contents of this document, including any conclusions or recommendations.

The use of or reliance on this document by any Third Party shall be at its own risk, and MHI accepts no responsibility or liability for the consequences of this document being used or relied upon by such Third Party. Any Third Party will, by such use or reliance, be taken to have confirmed its agreement to:

- (a) Indemnify MHI, its affiliates, and any person or entity acting on their behalf (“Indemnitees”), for all losses, costs, damages or expenses suffered or incurred by the Indemnitees as a result of such Third Party’s use or reliance on this document; and
- (b) Release the Indemnitees from any and all liability for direct, indirect, special or consequential damages (including but not limited to loss of revenue or profit, lost or damaged data, loss of goodwill or other commercial or economic loss) suffered or incurred by the Third Party, or for those at law for whom it is responsible, as a result of its or their use or reliance on this document whether based in contract, warranty or tort, (including but not limited to negligence), equity, strict liability or otherwise.

## Contents

1	Executive Summary .....	5
1.1	Objectives.....	5
1.2	Methods .....	5
1.3	Results .....	5
1.4	Conclusion .....	5
2	Introduction.....	6
3	Methodology .....	8
4	Study Model.....	8
4.1	Study Lines .....	10
4.2	Synchronous Machine Models .....	10
4.3	Type 3 Generic Windfarms .....	12
4.4	Type 4 Generic Windfarms .....	13
4.5	HVDC Model .....	15
4.6	Network Equivalent Model .....	15
4.7	Assumptions and Limitations of Full Network Model .....	16
5	Protection Elements .....	17
5.1	PSCAD™ Distance Protection Model.....	17
5.1.1	Distance Relay Theory .....	18
5.1.2	Differences between Modelled and Real Relays.....	19
5.1.3	Mho Element Algorithm Details .....	19
5.1.4	Potential Issues.....	21
5.2	PSCAD™ Over-current Protection Model.....	24
5.2.1	Potential Issues.....	24
5.3	PSCAD™ Differential Protection Model .....	25
5.3.1	Potential Issues.....	25
6	Fault Studies.....	26
6.1	400 kV Branxton to Wishaw .....	26
7	Note: Please see References .....	26
7.1.1	Impedance Over-reach during weak fault conditions .....	27
7.2	132 kV Innerwick to Dunbar.....	30
7.2.1	Effect of Polarization Settings on Zone 1 Detection .....	30
8	Effect of Differential Protection on Mal-operations.....	32
9	Power Angle Swings.....	32
10	Impact on Negative Sequence Functions.....	34
11	Impact on Rate-Of-Change-Of-Frequency and Vector Shift Relays .....	35
11.1	Rate-Of-Change-Of-Frequency (ROCOF) Relay .....	35

11.2	Vector Shift (VSR) Relay .....	37
12	Conclusion .....	38
13	Next Steps.....	39
14	References.....	40

# 1 Executive Summary

## 1.1 Objectives

The objective of this study is to investigate the effect on performance of AC protection systems in a weakening network. As large synchronous machines are retired in the UK network and the number of converter-based plants increases (i.e. Onshore/Offshore Wind, HVDC, Solar, Battery, etc.) the level of fault current and inertia will steadily decrease [1]. These quantities are critical to the design and security of current protection systems. This study tests and identifies several potential issues in a representative portion of the network.

## 1.2 Methods

A detailed PSCAD™ model of the network around Torness Power Station was developed including detailed generic EMT models for nearby wind farms (full converter models with power electronic switches) and synchronous machines. Generic protection elements were added to the model and a variety of faults were applied under various network conditions. The outputs of the protection relays were studied for potential mal-operations.

## 1.3 Results

Mal-operations for distance protection elements were observed when system strength is decreased (through the retirement of the Torness Power Station and disconnection of certain critical lines). Increased oscillations in the current and voltage during fault conditions cause a protection over-reach and premature tripping of the protected equipment. In addition, zone over-reach was identified in connection with the memory polarization function for one case.

High levels of Rate-of-Change-of-Frequency were also observed. While not a factor in the transmission level protection, it can be a factor in the disconnection of distributed generation (small scale generators at the low voltage level of the network).

No other functions mal-operated in the cases tested but potential issues are highlighted in the remaining sections.

## 1.4 Conclusion

Some potential causes of mal-operation were investigated and could compromise the security of the UK network now and in the future. Furthermore, the level of detail normally specified for protection models in studies (both traditional and EMT such as PSCAD™) is insufficient to catch all potential mal-operations at the functional level. More data and detail in models (including manufacturer models) will be required to confirm the operation of protection in the National Grid ESO.

## 2 Introduction

As the number and capacity of inverter-based devices increases in a network, the fundamental assumptions of the electrical system response to disturbances may no longer be valid. These sources are rapidly increasing their percentage of generation on a day-to-day basis but do not give the same characteristics as the classical generation during the disturbances. Classical synchronous generators can provide many times (often  $\times 10$ ) rated current during nearby faults and supply significant negative and zero sequence current for unbalanced fault types.

In comparison to conventional synchronous machines, inverter based generation is typically limited to produce at most 1.1 pu of rated load current during fault conditions for a shorter period of time but can also provide that current out of phase with the residual voltage of the network relating to the PLL-enabled current loops struggling to track the sudden changes in network voltage angle and magnitude occurring across fault conditions. As sources are replaced, the total system fault level decreases, but also the behaviour during the fault becomes less predictable. Additionally, the envelope of the fault current is not guaranteed to look the same as protection engineers are accustomed to and may not contain the same ratios of sequence currents. Inverter based generators are not traditional providers of system inertia as well. This significantly affects the overall frequency deviation for most disturbances. A typical control system will act too slowly to contribute to system stability though significant work and demonstrations are currently being undertaken to modify control systems such that inverter-based generators can significantly improve post disturbance frequency response. This functionality is not typically available in previously installed plants.

Existing transmission protection solutions are defined based on classical behaviours of synchronous machines in response to an AC system fault. Common approaches include over-current protection (responding to scale of fault current detected in an escalating speed depending on the magnitude), differential protection (identifying a change of current direction towards a faulted element covered by the associated relays) and distance protection (utilizing impedance-based methods to identify the location of a fault and a graded protection response across overlapping distance protection “zones” to respond to a fault). Each application of these will include digital or electromechanical relay settings, whose settings and algorithms have been defined in the past based on classical assumptions on how fault current will manifest within a given fault condition upon a given circuit within the transmission network. This study focusses on distance protection primarily, and is intended to review how the detailed protection models within PSCAD may capture and respond to these changes in fault current now beginning to be observed.

In the following sections, the aforementioned fault current reduction and inertia reduction are discussed with respect to the protection aspects of the different relay types and functions as modelled in PSCAD™.

In this work, a representative system is studied in and around Torness Nuclear Power Station and seeks to establish the effects on protection due to future changes to network configuration in the area, including the retirement of Torness Generators 1 and 2. This area was selected due to the potential for low fault level conditions in the now and in the future.

The initial network model information was provided to MHI in the form of a reduced PowerFactory™ case. Dynamic plants were represented using generic plants from PSCAD™ that include detailed inverters and control loops. Protection is represented with generic PSCAD™ models which reflect the existing protection settings provided. A variety of fault locations and resistances were explored and relevant mal-operations are commented on.

### 3 Methodology

A detailed PSCAD™ model of the network around Torness Power Station was developed including detailed generic EMT models for nearby wind farms (full converter models with power electronic switches) and synchronous machines (detailed differential machine equations with exciter controls). Transmission lines were represented using frequency dependent representations (Bergeron model) where the electrical travel time of the line is greater than the simulation time step (20  $\mu$ s). Short lines were represented using a Coupled Pi Model. Generic protection elements were added to the model and a variety of faults were applied under various network conditions. The outputs of the protection relays were studied for potential mal-operations.

A high level of detail is required in the PSCAD™ model to represent the in-fault behaviour of the converter-based generation. In addition, a detailed generic protection model is used to get the best possible results without directly testing with manufacturer created models.

The elements of the model are discussed in more detail in the following section.

### 4 Study Model

The study model contains network elements in and around the Torness Nuclear Power Station in the SP Transmission area of the Great Britain transmission network. The primary direction of modelling is south and west along the Torness to Strathaven corridor shown in Figure 1. Dynamic devices located near study lines were modelled using generic PSCAD™/EMTDC models with representative parameters. The completed PSCAD™/EMTDC model is shown in Figure 2 to Figure 8.

The included models are as follows:

- A) Synchronous Machines:
  - Torness 1 & 2
- B) Type 3 Windfarms (Doubly Fed Induction Generators)
  - Aikengall WF
  - Crystal Rig WF
  - Fallago Rig WF
- C) Type 4 Windfarms (Full Converter Generators)
  - Aikengall II WF
  - Crystal Rig II WF
  - Branxton WF
  - NNGB WF
- D) VSC HVDC
  - North Sea HVDC Link



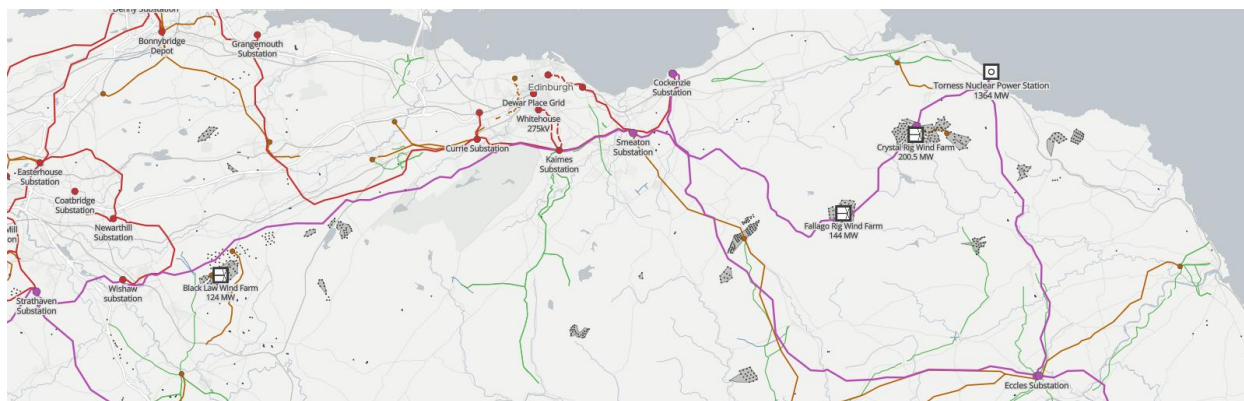


Figure 1: Torness Area Map

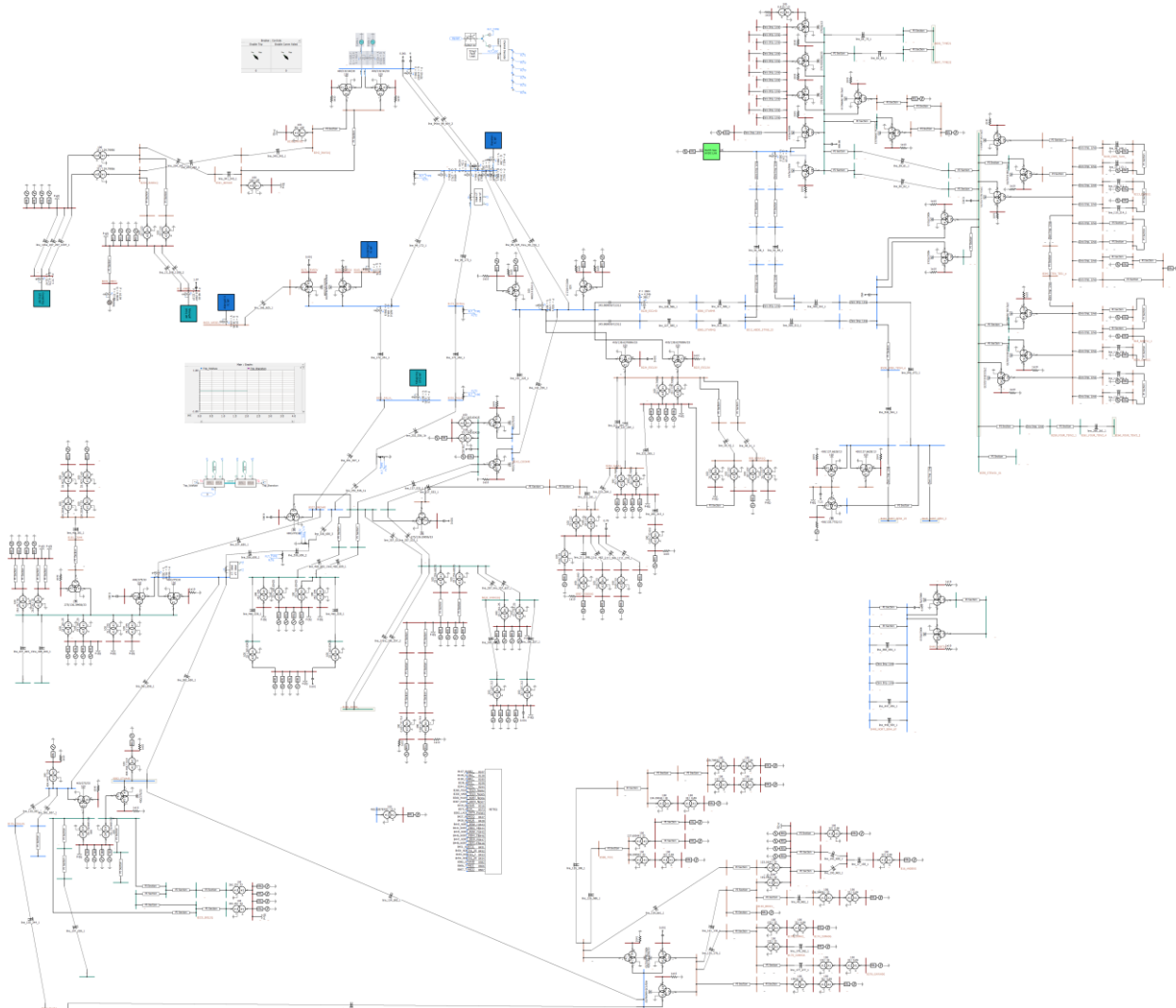


Figure 2: PSCAD™ Dynamic Model Representation of Torness Area Model

## 4.1 Study Lines

For the purposes of this report two lines were studied in detail:

- 1) 400 kV Branxton to Wishaw (Currently Torness to Strathaven)
- 2) 132 kV Innerwick to Dunbar

Both lines were represented as Bergeron frequency-dependent models with RXB data extracted from the provided PowerFactory™ model.

Note: Please see References

[1] "National Trends and Insights (A System Operability Framework Document)", National Grid ESO,  
<https://www.nationalgrideso.com/document/190151/download>

[2] J. Holbach, R. Zhang, T. Charton, D. Kerven and S. Ward, "Protection functionality and performance with declining system fault levels and inertia within national grid electricity transmission system in the United Kingdom," 15th International Conference on Developments in Power System Protection (DPSP 2020), 2020, pp. 1-6, doi: 10.1049/cp.2020.0065.

[3] "Distance Relay Fundamentals", GE Power Management, GER-3966,  
<https://www.gegridsolutions.com/products/applications/ger3966.pdf>

[4] Xue, Y., Douglas I. Taylor and Yu Xia. "Line Differential Protection Under Unusual System Conditions." (2015). [https://cms-cdn.selinc.com/assets/Literature/Publications/Technical%20Papers/6568\\_LineDifferential\\_BK\\_20120904\\_Web.pdf?v=20201215-234228](https://cms-cdn.selinc.com/assets/Literature/Publications/Technical%20Papers/6568_LineDifferential_BK_20120904_Web.pdf?v=20201215-234228) and **Error! Reference source not found.** for settings details.

## 4.2 Synchronous Machine Models

The nuclear power generators at Torness are modelled as synchronous machines. Machine parameters were supplied in Generator Data format. The required data parameters and units are shown in Table 1.

*Table 1: Required Data for Synchronous Machine*

Parameter	Unit
Rated RMS Line-to-Neutral Voltage	kV
Rated RMS Line Current	kA
Base Angular Frequency	Hz
Inertia Constant	s
Armature Resistance [Ra]	pu
Potier Reactance [Xp]	pu
D: Unsaturated Reactance [Xd]	pu

D: Unsaturated Transient Reactance [Xd_]	pu
D: Unsaturated Sub-Transient Reactance [Xd__]	pu
D: Unsaturated Transient Time (Open) [Td_]	s
D: Unsaturated Sub-Transient Time (Open) [Td__]	s
Q: Unsaturated Reactance [Xq]	pu
Q: Unsaturated Transient Reactance [Xq_]	pu
Q: Unsaturated Sub-Transient Reactance [Xq__]	pu
Q: Unsaturated Transient Time (Open) [Tq_]	s
Q: Unsaturated Sub-Transient Time (Open) [Tq__]	s

No information was available in detail for exciter or governor model and as such some approximations are made. The governor control is assumed to be fixed during the duration of the fault and the exciter is modelled using a generic AC1A model.

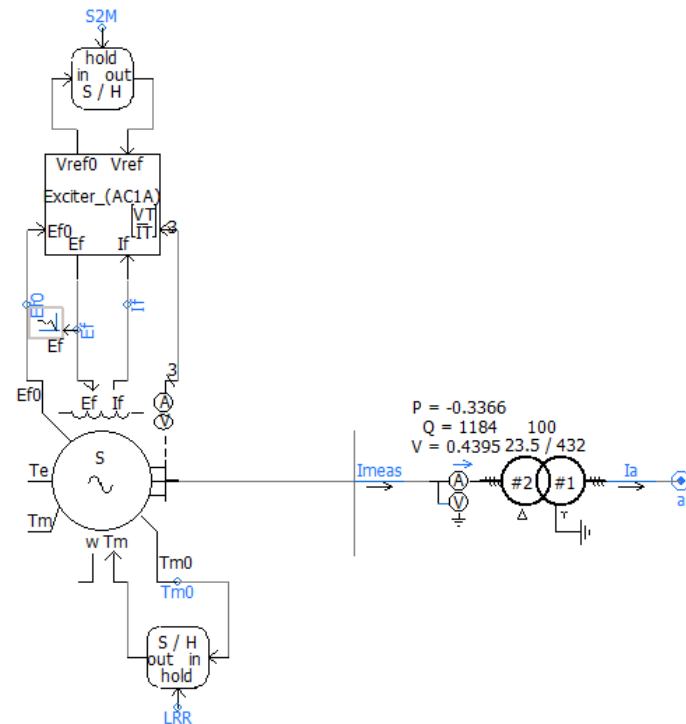


Figure 3: Torness Plant Generic Schematic

### 4.3 Type 3 Generic Windfarms

Type-3 wind turbine generators (WTG) also known as Doubly-Fed Induction Generators (DFIG) can be modelled in the form of two separate systems - mechanical and electrical - as shown in Figure 4. The mechanical system extracts the requested power from the wind and yields mechanical torque. The electrical system converts the mechanical torque to the electrical one and thus electric power. The interface between mechanical and electrical systems is the induction machine (IM), which converts the mechanical energy into electrical energy. Since the effect of wind variation is much slower than the time frame of a typical fault the pitch angle controller and blade physics formulae are replaced with a simple PI controller that controls input torque to the induction machine. The mechanical and electrical systems shown in Figure 5 are represented by the following components.

1. Mechanical System consists of:
  - Induction Machine (Also Electrical)
  - Simple PI Torque Controller
2. Electrical System consists of:
  - Grid-side Converter and Controls
  - Rotor-side Converter and Controls
  - DC-link Chopper Protection
  - Crowbar Protection
  - Low Pass Filter
  - 3-Winding Grid Transformer
  - Power Scaling Component (see Figure 5)

All converters in the model are fully realized with dynamic two-level converters for both grid- and rotor-sides and are developed based on IGBT semiconductor switches.

Additionally, a simple Power Park Controller (PPC) is used to generate per-unitized active and reactive power targets referenced to the Point-of-Connection (POC) which are passed to the wind turbine controller.

This model represents the following wind farms using a generic model:

- Aikengall I
- Crystal Rig I
- Fallago Rig

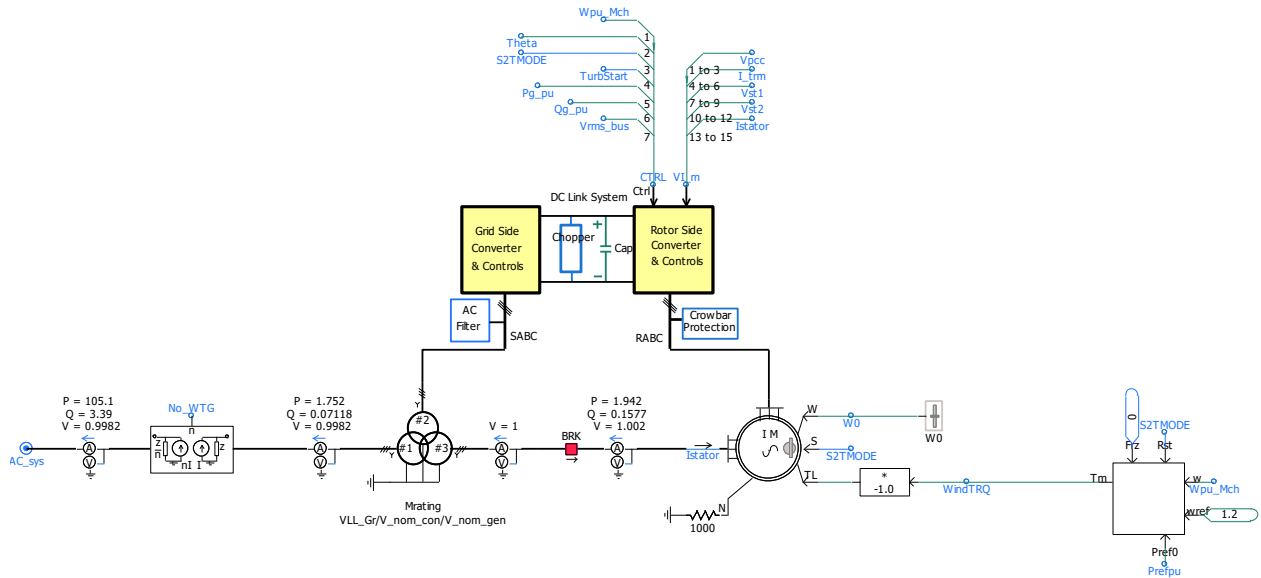


Figure 4: Generic Type III Wind Farm Model

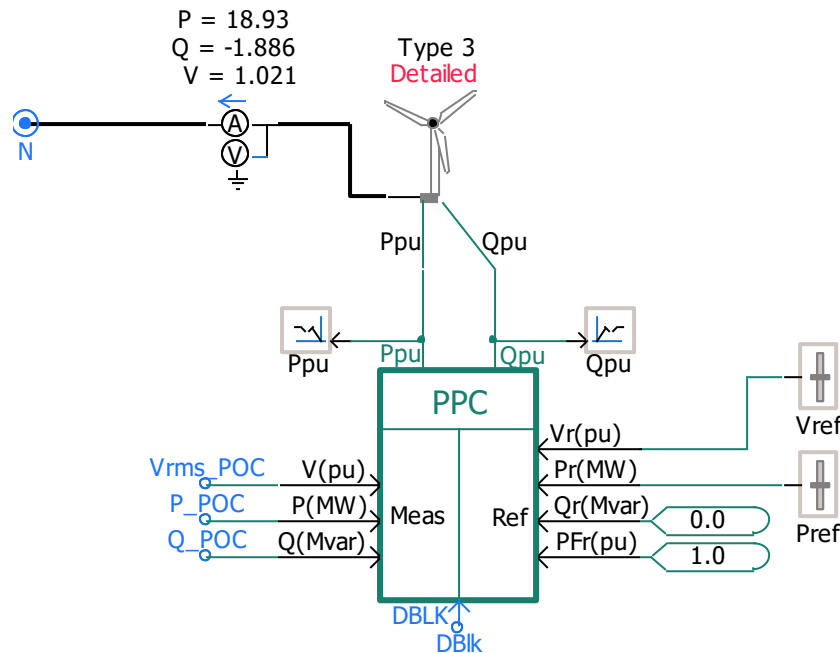


Figure 5: Generic Type III Windfarm with Power Park Controller

#### 4.4 Type 4 Generic Windfarms

The Type-4 wind turbine generator is similarly modelled in the form of two separate systems - mechanical and electrical – as shown in Figure 6. The mechanical system extracts the requested power from the wind and yields mechanical torque. The electrical system converts the mechanical torque to the electrical one and thus electric power. The interface between mechanical and electrical systems is the permanent magnet machine (PM), which converts the mechanical energy into electrical energy and passes it through the full converter. Since the effect of wind variation is much slower than the time frame of a typical fault the pitch angle controller and blade physics formulae are replaced with a

simple PI controller that controls input torque to the permanent magnet machine. The mechanical and electrical systems shown in Figure 6 are represented by the following components.

3. Mechanical System consists of:
  - Permanent Magnet Machine (Also Electrical)
  - Simple PI Torque Controller
4. Electrical System consists of:
  - Grid-side Converter and Controls
  - Machine-side Converter and Controls
  - DC-link Chopper Protection
  - Low Pass Filters
  - LV/MV Power Transformer
  - Power Scaling Component (see **Error! Reference source not found.**)

All converters in the model are fully realized with dynamic two-level converters for both grid- and rotor-sides and are developed based on IGBT semiconductor switches.

Additionally, a simple Power Park Controller (PPC) is used to generate per-unitized active and reactive power targets referenced to the Point-of-Connection (POC) which are passed to the wind turbine controller.

This model represents the following wind farms using a generic model:

- Aikengall II
- Branxton
- Crystal Rig II
- NNGB

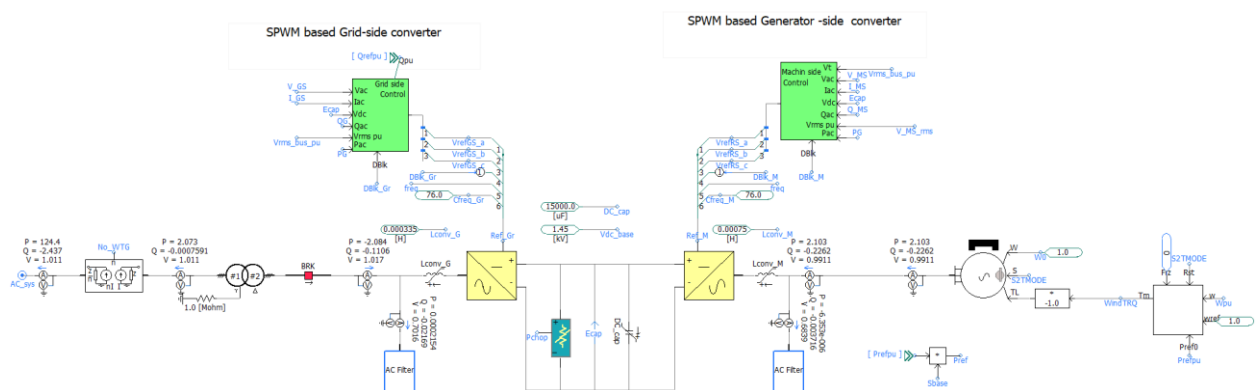


Figure 6: Generic Type IV Wind Farm Model

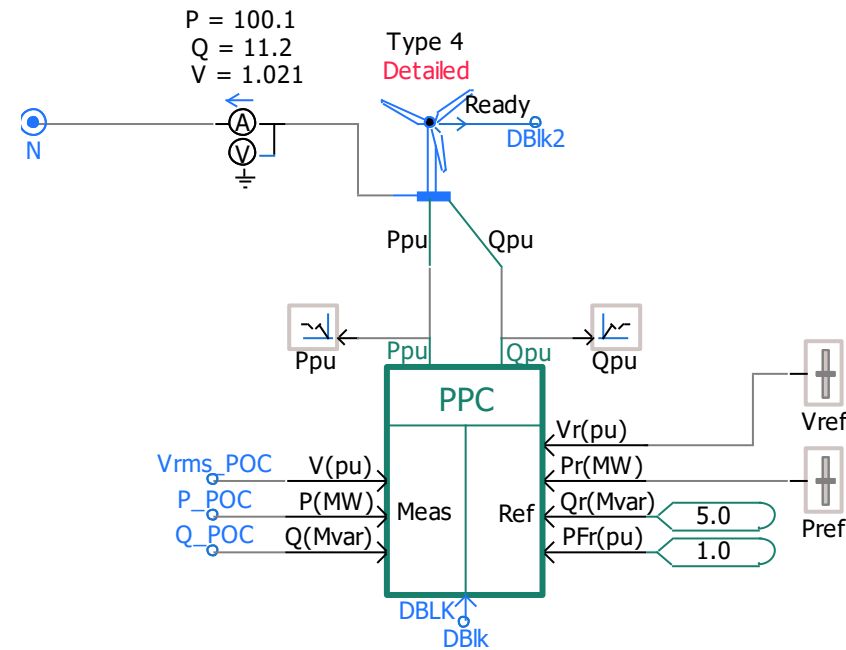


Figure 7: Generic Type IV Windfarm with Power Park Controller

## 4.5 HVDC Model

The future plant, North Sea HVDC Link between Blyth in the UK and Norway, is modelled using a detailed generic VSC model. Terminals are represented using a Modular Multilevel topology with decoupled current controllers. At Blyth the reactive power and DC voltage are held steady while at the Norway side active and reactive power is controlled.

The grid configuration at the Norway side of the model is outside the scope of the study and as such is represented as strong voltage source so as to not contribute any additional interactions.

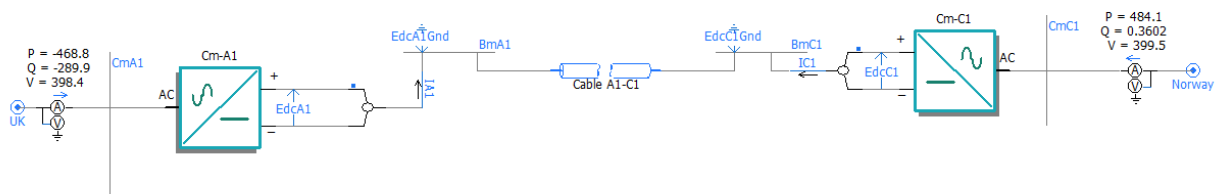


Figure 8: North Sea HVDC Link Model

## 4.6 Network Equivalent Model

For the remaining network components beyond the boundary of the identified study area, it is represented by numerically reducing the admittance matrix to ensure that the load flow and short circuit levels are maintained.

Network equivalencing was carried out by SPT in PowerFactory™ prior to the network information being provided to MHI. Some elements inconsistent with EMTDC simulation (negative resistance in loads/branches) were disabled.

After the model was fully implemented the short circuit levels and power flow levels were compared between the existing RMS Powerfactory™ model and the new PSCAD™ model. Results are shown in Table 2 and Table 3 below.

*Table 2: 3-Phase Short Circuit Model Comparison*

Bus	PowerFactory™ [kA]	PSCAD™ w/ Dynamics [kA]	Error
TORN4-	26.74	24.69	7.7%
BRNX4-	26.95	24.83	7.9%
CRYR4A	20.54	19.37	5.7%
FALL4A	17.41	16.89	3.0%
SMEA4Q	15.15	14.77	2.5%
CRYR4-	21.63	19.69	9.0%
ECCL4A	20.77	19.95	3.9%
WISH4-	30.04	28.51	5.1%
HEDD_STWB_23	27.16	25.50	6.1%
BLYT41	22.92	20.30	11.4%
STEW41	29.89	28.08	6.1%

*Table 3: Power Flow Model Comparison*

Bus		PowerFactory™		PSCAD™	
From	To	P [MW]	Q [Mvar]	P [MW]	Q [Mvar]
ECCLA4A	BRNX4-	-1281.3	-145.0	-1310.0	-145.0
TORN4-	BRNX4-	588.4	327.7	584.4	328
BRNX4-	CRYR4A	-79.5	96.4	-126.5	122.3
CRYR4-	FALL4-	-325.5	181.1	-366.9	207.1
WISH4-	SMEA4R	-189.4	-94.1	-132.5	-116.7

## 4.7 Assumptions and Limitations of Full Network Model

The model presented in this work is only for demonstration purposes and cannot be used to make detailed policy decisions. Due to a lack of information pertaining to specific manufacturer models during development the specific responses of all generic dynamic devices and protection algorithms are not guaranteed to match those found in the actual network.



## 5 Protection Elements

The main focus of this study was on the operation of the distance protection as this is the most common protection type at the Transmission voltage level. Also it is typically more prone to mal-operation than other transmission line protection types.

Other protection types such as Bus, Transformer, and Generator were deemed outside of the scope of this project due to a lack of relevant information at the time.

### 5.1 PSCAD™ Distance Protection Model

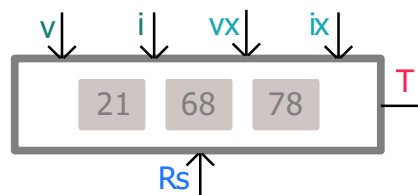


Figure 9: PSCAD™ Distance Protection Model

The distance protection relay module models the ANSI 21 protection capabilities and its ancillary functions. This relay module has four mho/quadrilateral protection zones supervised by out-of-step blocking, directional supervision, fault type identification, and load encroachment supervision functions (Note: though these functions are available not enough information was known about the supervisory function parameters that will be present in the future network arrangement to use these. Basic Mho protection zones are assumed). The external inputs/outputs to the model are:

Table 4: Description of External Ports

Port	Type	Description
v	Real(3)	Three phase voltage input. Intended for a three dimensional signal containing the secondary voltages of phases A, B and C, coming from voltage transformers (VTs) or a capacitive voltage transformer (CVTs). Units can be V or kV.
i	Real(3)	Three phase current input. Intended for a three dimensional signal containing the secondary currents of phases A, B and C, coming from current transformers (CTs). Units can be A or kA.
vx	Real(3)	Three phase auxiliary voltage input. Intended for a three dimensional signal containing three secondary voltages. If all or some of the inputs are unused, create a real signal with matching dimensions with zeros for the unused elements. Units should be the same as in input 'v'.
ix	Real(3)	Three phase auxiliary current input. Intended for a three dimensional signal containing three secondary currents. Generally used for providing ground ( $3I_0$ ) currents of parallel lines for compensation and/or zero sequence current for directional element. If all or some of the inputs are unused, create a real signal with matching dimensions with zeros for the unused elements. Units should be the same as in input 'i'.
RS	Integer	Reset signal. A binary signal (0 = normal operation, 1 = reset) that can be used to reset the relay trip signals and pickup signals.
T	Integer(4)	Trip signal output of relay. Used to disconnect phases of breaker.

The user can activate any number of zones and can use any combination of Mho and Quadrilateral schemes. Each supervisory function can be enabled/disabled separately, and trip logic can be configured.

Signal processing within the component include anti-aliasing filtering, Direct Current (DC) removal filtering, and selection of samples-per-cycle.

Additional options are provided for a variety of measurement polarization techniques (Memory, Cross, Positive Sequence, Positive Sequence Memory). This functionality ensures that there is a record of the measured signal that can be used for logic decisions even if the signal becomes almost zero during the fault disturbance.

### 5.1.1 Distance Relay Theory

Distance relays measure the terminal voltage and line current and determine impedance seen by the relay using ohm's law ( $V = IZ \therefore Z = \frac{V}{I}$ ). This impedance is compared to several different impedance elements (called zones) which are set based on the line impedance of the protected line. Protection zones are traditionally found in one of two shapes; mho (circle) or quadrilateral (rhombus). When the measured impedance crosses into and remains in a protection zone for a specified period of time a tripping signal is raised. Figure 10. shows a mho type zone and Figure 11 shows a quadrilateral type zone in the complex impedance plane.

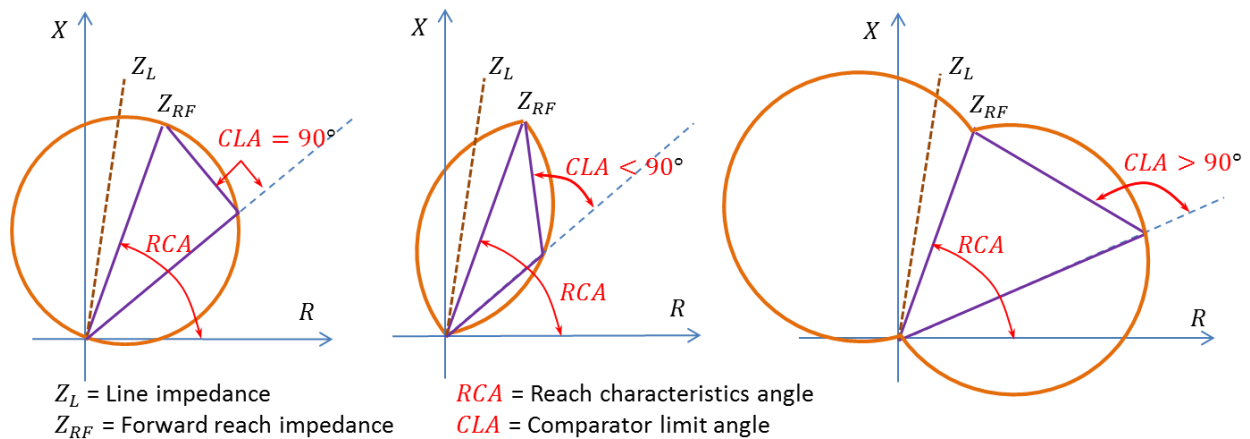


Figure 10: Mho Distance Element with Directional Lensing ( $CLA < 90$  degrees and  $CLA > 90$  degrees are typically known as lens and tomato type characteristics respectively)

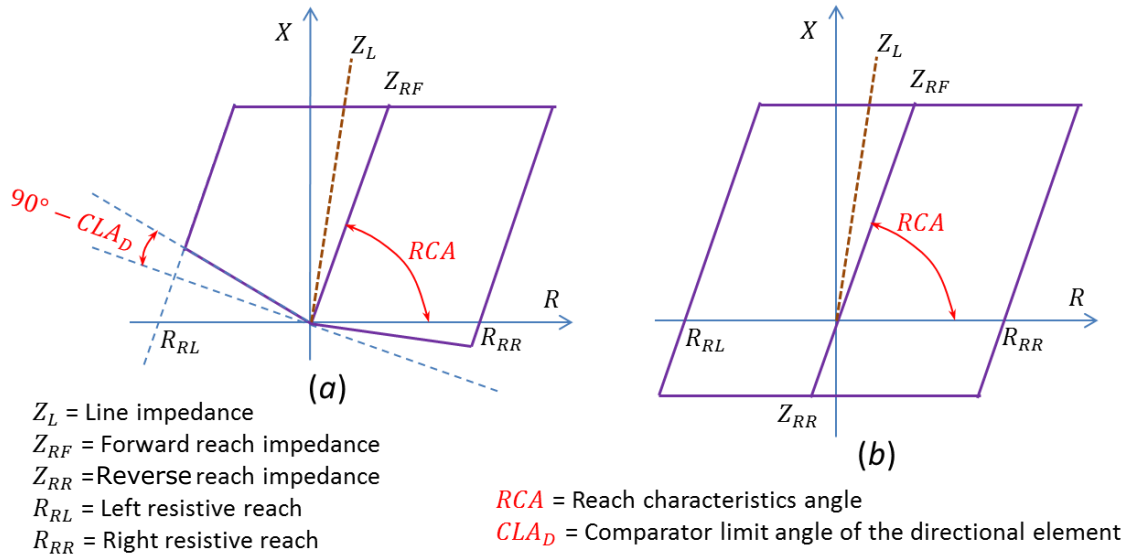


Figure 11: Quadrilateral Distance Element

### 5.1.2 Differences between Modelled and Real Relays

While modelled relays contain many of the same functions as the physical relays, many intricate details of each manufacturer's algorithms are unknown due to Intellectual Property. These changes can be as simple as additional delay blocks in the relay logic, or the much more complicated differences in how the relay processes the measured signals before being passed to the decision-making algorithms.

For detailed analysis of relay operation, it is preferred to use a full manufacturer provided model when available.

### 5.1.3 Mho Element Algorithm Details

While Mho distance elements are typically shown in the R-X plane for illustrative purposes, typical algorithms use a vector angle comparison method in the V ( $I \cdot R - I \cdot X$  rather than R-X) plane to determine in/out of zone status. The vectors use are shown in Table 5 below.

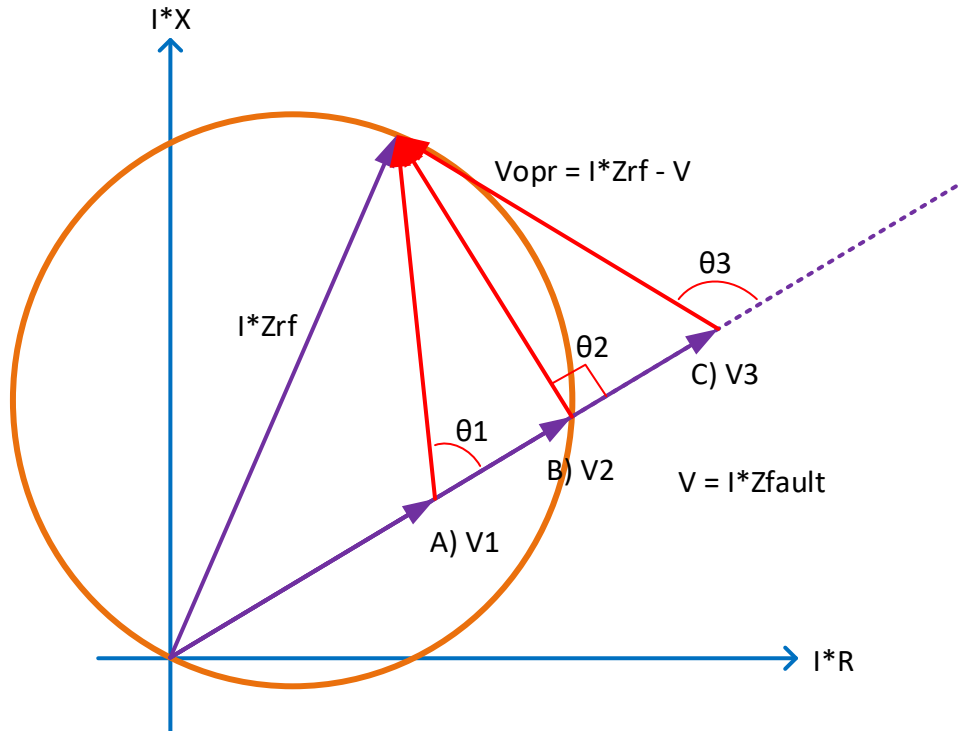
Table 5: Method of realization of directional Mho characteristics

Element	Vector-1	Vector-2
AB Phase	$(I_A - I_B) \cdot Z_{RF} - (V_A - V_B)$	$(V_{Apol} - V_{Bpol}) - (I_A - I_B) \cdot Z_{RR}$
BC Phase	$(I_B - I_C) \cdot Z_{RF} - (V_B - V_C)$	$(V_{Bpol} - V_{Cpol}) - (I_B - I_C) \cdot Z_{RR}$
CA Phase	$(I_C - I_A) \cdot Z_{RF} - (V_C - V_A)$	$(V_{Cpol} - V_{Apol}) - (I_C - I_A) \cdot Z_{RR}$
A Ground	$I_{A,Comp} \cdot Z_{RF} - V_A$	$V_{Apol} - I_{A,Comp} \cdot Z_{RR}$
B Ground	$I_{B,Comp} \cdot Z_{RF} - V_B$	$V_{Bpol} - I_{B,Comp} \cdot Z_{RR}$
C Ground	$I_{C,Comp} \cdot Z_{RF} - V_C$	$V_{Cpol} - I_{C,Comp} \cdot Z_{RR}$

The voltages used in Vector-2 depend on the polarization settings. For an example,  $V_{Ap0l}$ ,  $V_{Bp0l}$ ,  $V_{Cp0l}$  will be substituted by the respective positive sequence voltages from the memory ( $V_{A1M}$ ,  $V_{B1M}$ ,  $V_{C1M}$ ), if positive sequence memory polarization is used.

For zone 1 and 2, reverse reach ( $Z_{RR}$ ) is intentionally set to zero in the relay algorithm.

These vectors are used to calculate a representative angle which can be used to determine in/out of zone status. As shown in Figure 12, the R-X zone characteristics are multiplied by the measured current during run time to transform it into the Voltage plane. The vector  $I \cdot Z_{rf}$ , where  $Z_{rf}$  is the forward reach characteristic and  $I$  is the measured current, will always bisect the characteristic circle. Using Thales's theorem we can determine if the measured polarizing voltage (Vector-2) falls within the characteristic which is the criteria for zone pick-up. Thales's theorem states a triangle that is formed between the diameter of a circle and any point on the circle will have an angle of 90 degrees at the point. This is shown as  $\theta_2$  in Figure 12. Vector math is used to determine the angle between Vector-1 (operating voltage) and Vector-2 (the polarizing voltage). When the angle is equal to or less than 90 degrees (or the user settable Comparator limit angle) than the fault is considered in zone.



$Z_{rf}$  = Forward reach impedance  
 $Z_{fault}$  = Fault impedance + line impedance to the fault  
 $V_{opr}$  = Operating voltage. Characteristic voltage – measured voltage  
 $VX$  = Measured voltage vector  
 $I$  = Measured line current  
 $\theta X$  = Angle between operating voltage and measured voltage

Any angle  $\theta$  less than  $90^\circ$  indicates as in zone measurement.

Figure 12:  $I^*R$  -  $I^*X$  Plane Representation of Mho Characteristics

## 5.1.4 Potential Issues

### 5.1.4.1 Decreased Short Circuit Levels

Lowering the short circuit level on a line protected by distance protection has a high potential for protection mal-operation. Lowering the fault current may cause the relay to not operate due to the fault current not exceeding the minimum pick-up current.

Additionally, with a lower short circuit level the measured voltage and current during the fault will be lower. Increasing the penetration of inverter based sources effectively increases the source impedance as compared to synchronous machines. The source impedance will act as a voltage divider with the line impedance in series with the fault impedance as shown in Figure 13. When the ratio of the source impedance to line impedance (SIR) increases the voltage

seen at the relay will decrease. As the voltage and current decrease the accuracy of the measurement becomes worse. A SIR of <30 is required by National Grid in order for distance protection to be used [2].

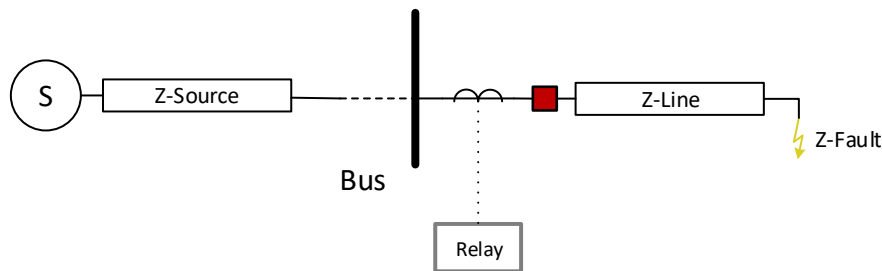


Figure 13: Source - Line Voltage Divider

$$SIR = \frac{Z_{source}}{Z_{line}}$$

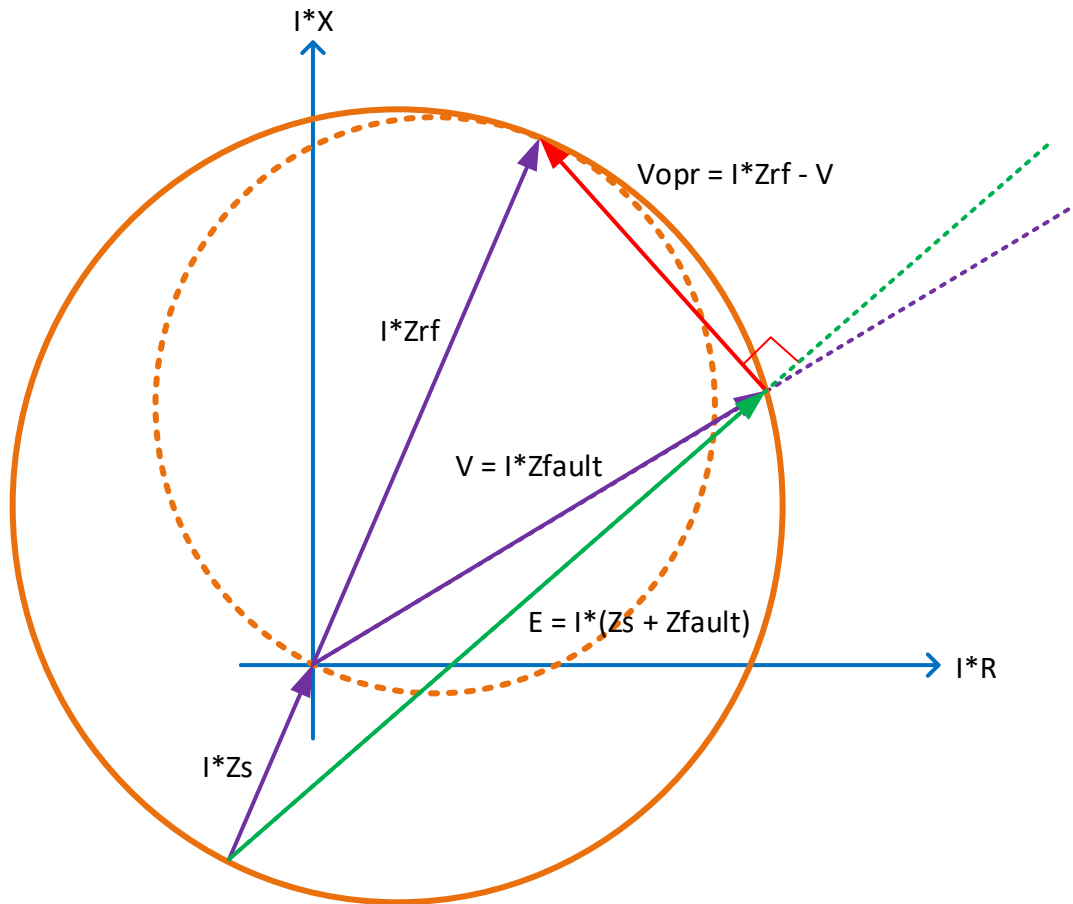
#### 5.1.4.2 Reduced System Inertia

The reduction of system inertia will generally increase the likelihood of power swings post fault. Without additional power swing blocking logic (not available in all older relays) impedance may swing into a protected zone of a non-faulted element. Additionally, a faster critical fault clearing time may be necessary to prevent system generation instability.

#### 5.1.4.3 Expanding Dynamic Characteristic

Distance relays that use voltage polarization provide additional security against extremely low voltage conditions by considering pre-fault voltages during the decision making logic.

As shown in Figure 14 the pre-fault voltage E has the effect of expanding the zone extents dynamically during fault inception [3]. This does not typically cause mal-operation but can if the memory parameters (length, hold duration, etc.) are not selected well. It can cause issues if the source impedance is large and the phase shift is large between pre and in-fault as the expansion is numerically dependent on these quantities.



$Z_{rf}$  = Forward reach impedance

$Z_{fault}$  = Fault impedance + line impedance to the fault

$Z_s$  = Source impedance

$V_{opr}$  = Operating voltage. Characteristic voltage – measured voltage

$V$  = Measured voltage vector

$E$  = Combination of measured voltage and prefault polarized voltage

$I$  = Measured line current

$\theta$  = Angle between operating voltage and  $E$

Any angle  $\theta$  between  $V_{opr}$  and  $E$  less than  $90^\circ$  indicates as in zone measurement. Using polarization prevents the measured voltage from being zero but can expand the zone if source impedance is high.

Figure 14:  $I^*R$  -  $I^*X$  Plane Representation of Mho Characteristics with Memory Polarization

## 5.2 PSCAD™ Over-current Protection Model



Figure 15: PSCAD™ Over-Current and Directional Over-Current Protection Models

While not a focus of this study (over-current relay is typically only used as backup protection for Transmission lines or at the low voltage level) over-current protection is also at high risk of mal-operation.

The standard over-current functions (ANSI 50,50N,51,51N) fall into two categories of algorithm:

- 1) Definite Time Over-Current – when the measured current exceeds the setting threshold for a prescribed period of time a trip signal is issued.
- 2) Inverse Time Over-Current – when the integral of the operating current exceeds a defined standard curve a trip signal is issued.

Directional over-current functions (ANSI 67,67N) add an additional algorithm to ensure that the direction of the fault current is considered rather than just the magnitude. This algorithm typically relies on the angles of the sequence currents to make a decision.

### 5.2.1 Potential Issues

All over-current relays rely on sufficient fault level to operate. As fault levels fall throughout the network there is a risk of inadequate fault current to issue a trip signal. Additionally, for directional over-current relays, many directional decision algorithms depend on the presence of certain sequence currents being present in expected amounts. These assumptions may no longer be true in the future configuration of the network.



### 5.3 PSCAD™ Differential Protection Model

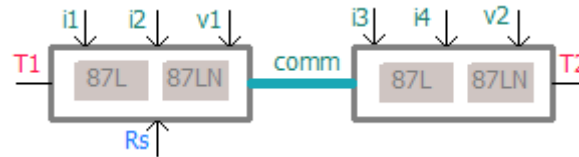


Figure 16: PSCAD™ Line Differential Protection Model

Differential current protection measures the current on each side of the protected equipment. Each side of the protected equipment sends the others the measured current and the values are summed (ANSI 87L,87LN). If the currents sum to a non-zero (or above some threshold) value a trip signal is issued.

#### 5.3.1 Potential Issues

Differential protection is generally resistant to low fault current but does rely on consistent communication between the relays at each end of the equipment. To avoid spurious trips from data corruption during communication a supplementary Disturbance detection function is typically employed [4]. It blocks the trip logic until a credible disturbance is detected. There are many designs for this function but most of them depend on some combination of the sequence currents and voltages which make them susceptible to changing network characteristics. Additionally, as the fault current reduces the operating magnitude may get closer to the bias setting (a blocking characteristic that prevents mal-operations due to error from line-charging current, CT error, or relay measurement error) which increases the risk of mal-operation.

## 6 Fault Studies

Faults were performed at various locations along each line, especially around the impedance zone boundaries. Three fault types were investigated in each case (ABC to Ground, AB to Ground, A to Ground).

### 6.1 400 kV Branxton to Wishaw

While the currently installed line configuration is terminated at Torness and Strathaven respectively, the planned configuration has additional connections at Branxton and Wishaw. This requires a re-implementation of current protection schemes. For the sake of this study the new protection parameters are assumed to be similar to the currently available ones.

The Line information for Branxton to Wishaw is as follows (Zone distances are selected based on the previous Torness to Strathaven protection information):

*Table 6: Branxton to Wishaw Line Information*

Line Info	
<b>Total Line Impedance</b>	38.1 $\angle 85.1^\circ \Omega$
<b>VT Ratio</b>	3636
<b>CT Ratio</b>	2000
<b>Secondary Impedance</b>	20.96 $\angle 85.1^\circ \Omega$
<b>Zone 1</b>	75%
<b>Zone 2</b>	117%
<b>Zone 3</b>	140%

The protection for this line is represented using the PSCAD™ Protection Library Distance Protection Module. In this study the protection is assumed to be identical at either end. All distance zones are represented as Mho characteristics with comparator limit angles set to  $90^\circ$  (no lens or tomato shape).

The aforementioned variety of faults (ABC to Ground, AB to Ground, A to Ground) were applied at each of the locations shown in Figure 17.

## 7 Note: Please see References

[1] "National Trends and Insights (A System Operability Framework Document)", National Grid ESO,  
<https://www.nationalgrideso.com/document/190151/download>

[2] J. Holbach, R. Zhang, T. Charton, D. Kerven and S. Ward, "Protection functionality and performance with declining system fault levels and inertia within national grid electricity transmission system in the United Kingdom," 15th International Conference on Developments in Power System Protection (DPSP 2020), 2020, pp. 1-6, doi: 10.1049/cp.2020.0065.

[3] "Distance Relay Fundamentals", GE Power Management, GER-3966, <https://www.gegridsolutions.com/products/applications/ger3966.pdf>

[4] Xue, Y., Douglas I. Taylor and Yu Xia. "Line Differential Protection Under Unusual System Conditions." (2015). [https://cms-cdn.selinc.com/assets/Literature/Publications/Technical%20Papers/6568\\_LineDifferential\\_BK\\_20120904\\_Web.pdf?v=20201215-234228](https://cms-cdn.selinc.com/assets/Literature/Publications/Technical%20Papers/6568_LineDifferential_BK_20120904_Web.pdf?v=20201215-234228) for settings details.

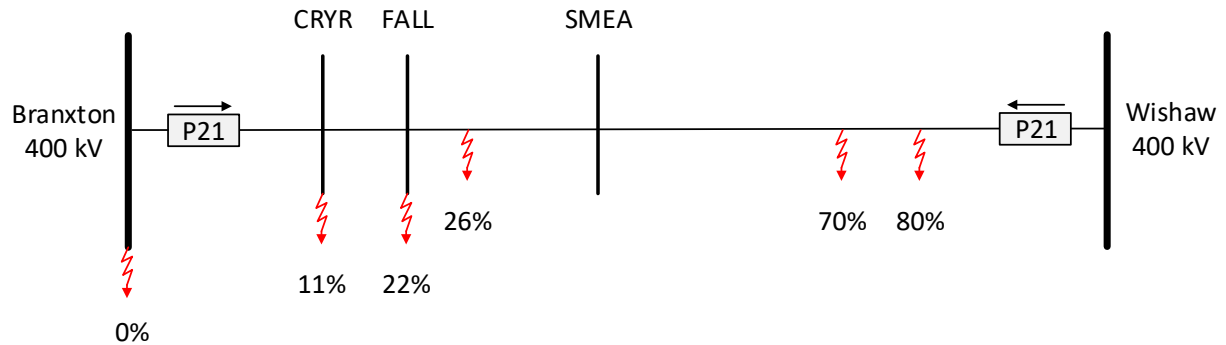


Figure 17: Branxton to Wishaw Fault Locations

### 7.1.1 Impedance Over-reach during weak fault conditions

A series of contingencies were investigated with decreasing levels of fault current:

- System normal, all power plants in service
- System normal, Torness 1/2 out-of-service
- N-1 one Branxton to Eccles line out, Torness 1/2 out-of-service
- N-2 both Branxton to Eccles line out, Torness 1/2 out-of-service
- N-2 both Branxton to Eccles line out, Torness 1/2 out-of-service, all WF out-of-service

Almost all scenarios did not show any mal-operations. The primary mal-operation occurred for faults at 80% of the line length. An incorrect Zone 1 fault is detected from the Branxton end of the line (Outside of zone 1 therefore overreach). Note the transient pickups (**bolded**) during a three phase to ground fault at 80% of the line length as shown in Figure 18.

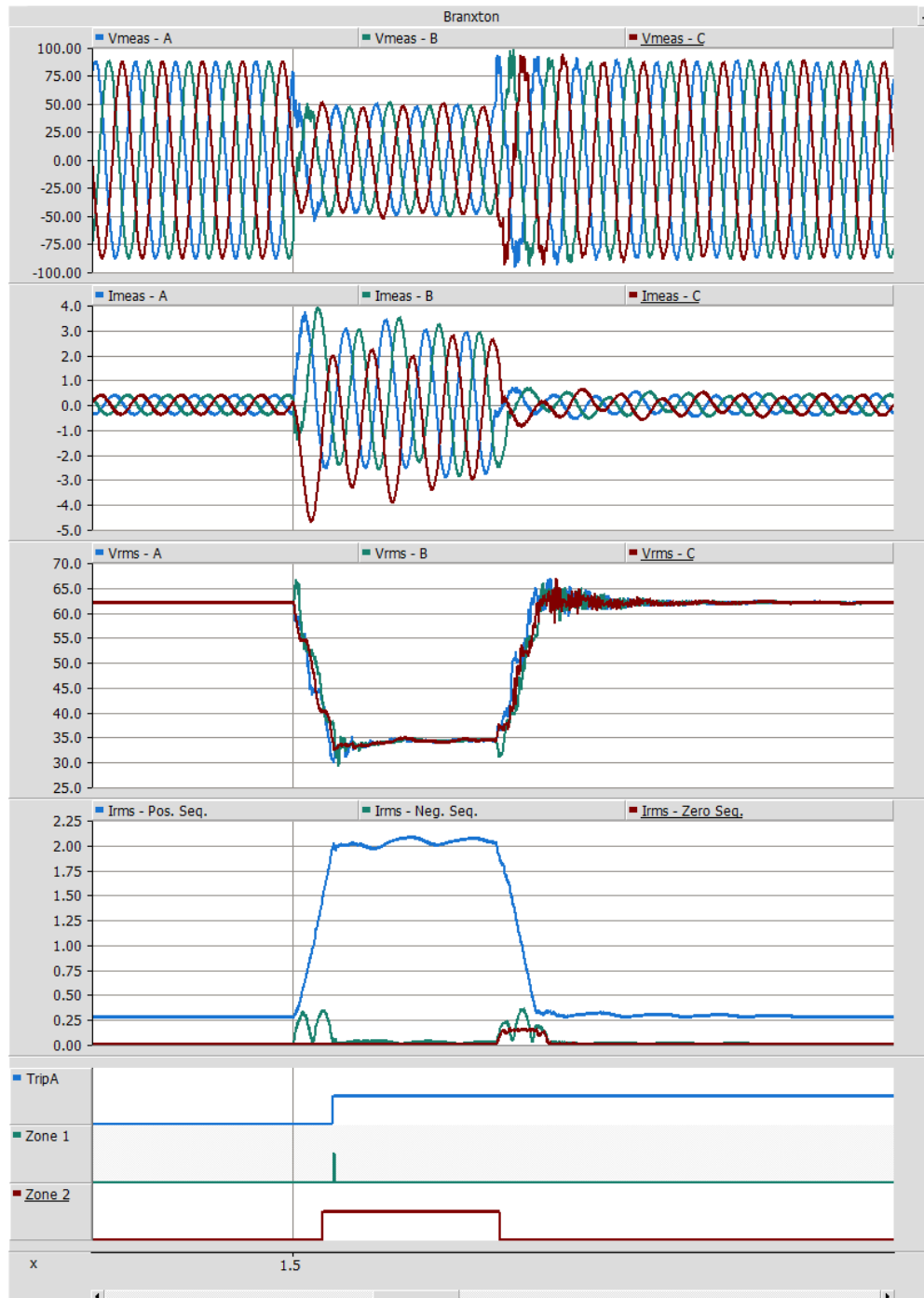
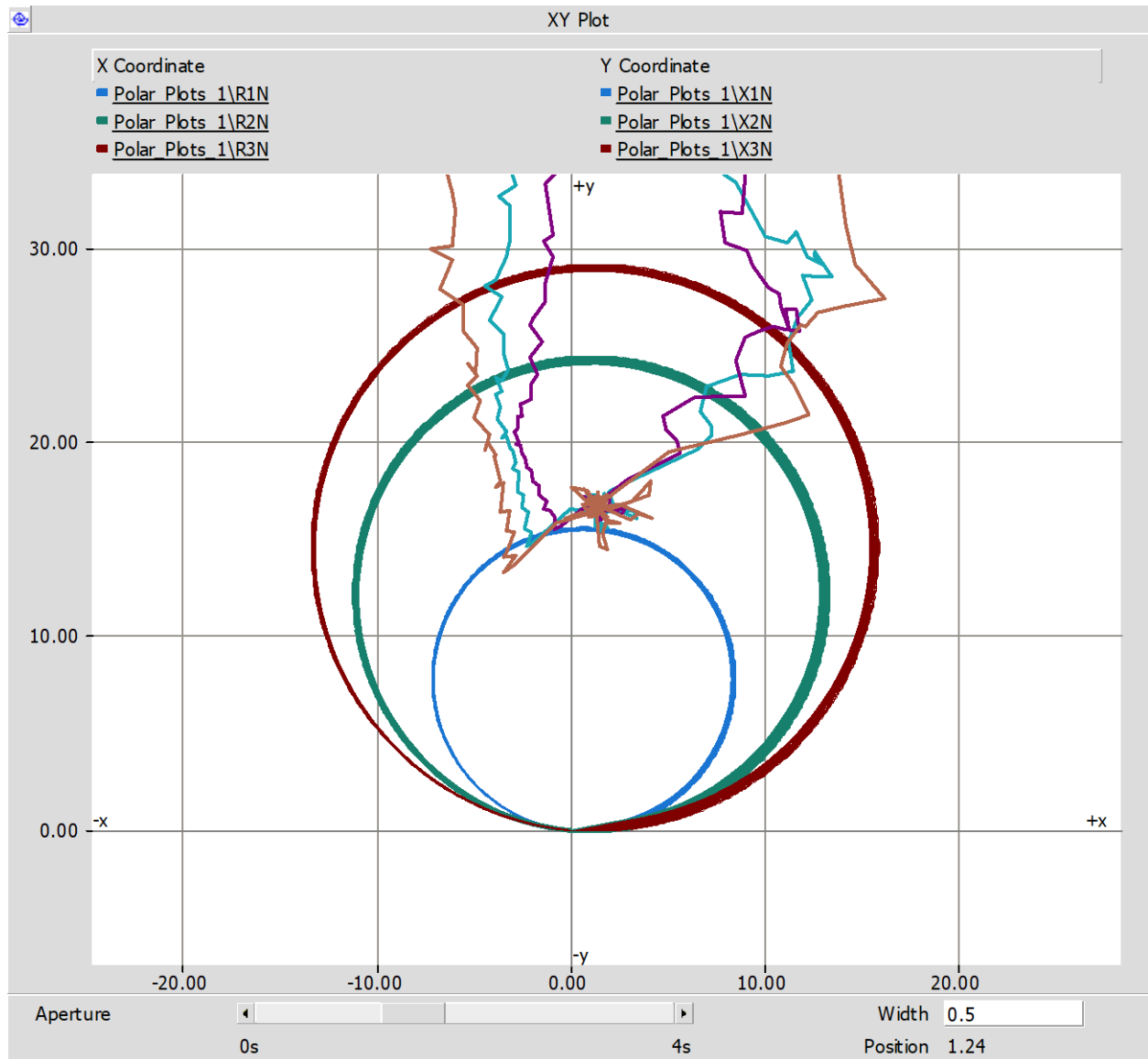


Figure 18: Measured Protection Signals showing Temporary Zone 1 pickup

The measured impedance swings temporarily into the Zone 1 Mho characteristic. Additionally, comparing the responses between several network conditions in Figure 19 shows the increased transient swing as the system strength decreases.



- System normal, all power plants in service
- System normal, Torness 1/2 out-of-service
- N-2 both Branxton to Eccles line out, Torness 1/2 out-of-service, all WF out-of-service

*Figure 19: Effects of decreasing fault level on impedance trajectory*

The likelihood of this issue occurring in practice will depend on the exact manufacturer implementation of the distance algorithm. Many relays will include hidden proprietary delays in the decision-making logic to prevent instantaneous tripping from tripping incorrectly. Due to the nature of the intellectual property it is unfeasible to attempt to determine these delays. Specific relay testing with potentially mal-operating conditions should be undertaken during the design phase to ensure correct operation.

## 7.2 132 kV Innerwick to Dunbar

One of the two 132 kV Innerwick to Dunbar lines was selected to test potential mal-operations for very low system strength that may occur in certain conditions after the disconnection of Torness Power Station.

The Line information for Innerwick to Dunbar is as follows (Zone distances are selected based on typical industry values):

Table 7: Innerwick to Dunbar Line Information

Line Info	
<b>Total Line Impedance</b>	3.82 $\angle 67.6^\circ \Omega$
<b>VT Ratio</b>	1200
<b>CT Ratio</b>	2000
<b>Secondary Impedance</b>	6.38 $\angle 67.6^\circ \Omega$
<b>Zone 1</b>	80%
<b>Zone 2</b>	120%

The protection for this line is represented using the PSCAD™ Protection Library Distance Protection Module. For the sake of this study the protection is assumed to be identical at either end. All distance zones are represented as Mho characteristics with comparator limit angles set to  $90^\circ$  (no lens or tomato shape).

Faults are applied approximately 10% of the line length measured from the Dunbar side.

Note: Please see for settings details.

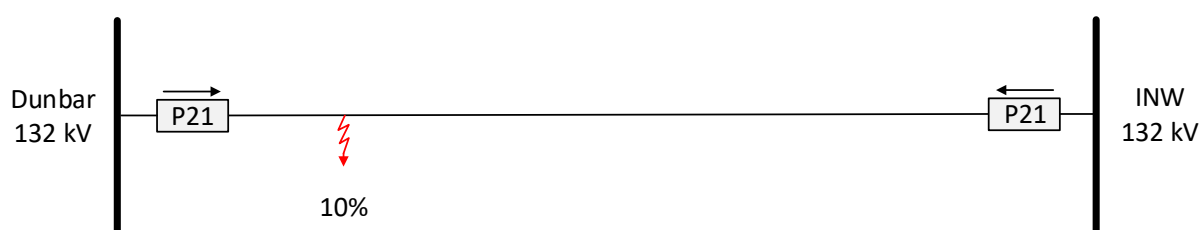


Figure 20: Innerwick to Dunbar Fault Location

### 7.2.1 Effect of Polarization Settings on Zone 1 Detection

During the fault initiated at approximately 10% of the line length from Dunbar the Innerwick relay has a temporary zone 1 pickup that results in an immediate trip signal. As mentioned in 5.1.4.3 Expanding Dynamic Characteristic the large source impedance coupled with a large phase angle jump cause the zone characteristic to expand dynamically for a short period of time during the fault inception. The expanded zone catches the measured impedance in zone 1.

Removing memory polarization eliminates this behaviour but at the cost of reduced security for solid faults. Polarization settings should be reviewed as the network strength is reduced due to plant retirement.

## 8 Effect of Differential Protection on Mal-operations

Replacing the distance protection relays with a generic differential protection on the previous lines simplifies the protection settings and eliminates the observed modes of mal-operation. No additional mal-operations were observed.

## 9 Power Angle Swings

Power angle swings occur when generators temporarily move away from synchronism during a disturbance. This can lead to sustained low frequency voltage and current oscillations. Under certain conditions the trajectory of the power swing can pass through all distance protection zones and initiate a trip.

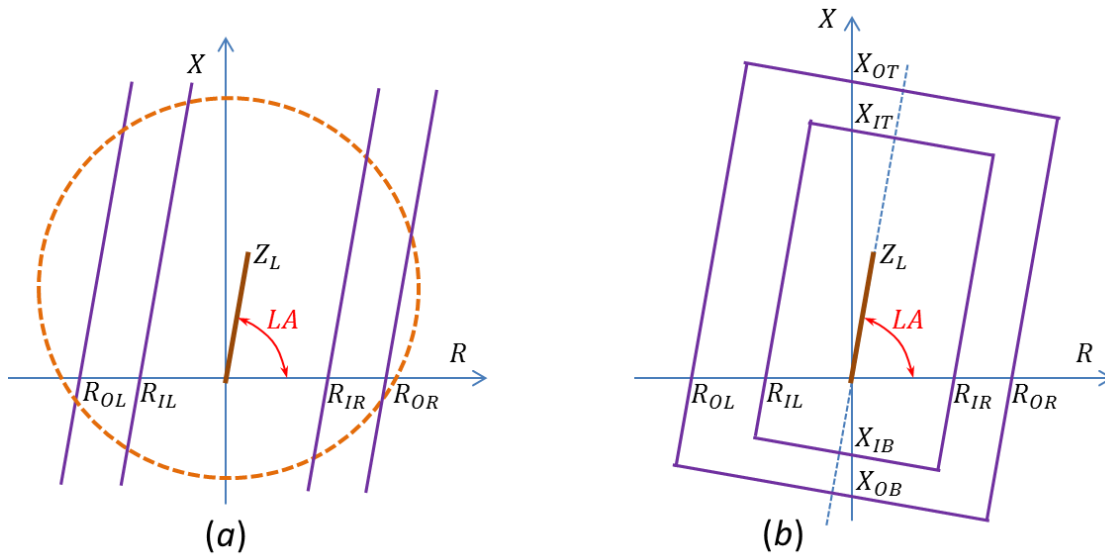
The Out-of-step (OOS) function can be used to detect stable power swings and out-of-step conditions in distance relays. It blocks selected distance protection elements during power swings or additionally can trip a line when an out-of-step condition is detected. The two most typical OOS schemes are shown in Figure 21.

The OOS function responds to measured positive sequence impedance. The power swing detection timers are started when the measured impedance enters the outer zone (or the area between outer blinders). If the measured impedance remains between the outer and inner zones (or between outer and inner blinders) until the relevant timer expires, a power swing condition is declared. The condition will persist until the measured positive sequence impedance leaves the outer zone (or blinder).

The speed of the impedance swing for an actual fault is significantly faster than a power swing and as such passes through the outer and inner zones (or between outer and inner blinders) before the timer expires. The power swing condition can either be used to block any zone trips or to cause a separate power swing condition trip.

No power angle swings were detected in the studied scenarios.





$Z_L$  = Line impedance  
 $R_{IL}$  = Inner zone left resistance reach  
 $R_{IR}$  = Inner zone right resistance reach  
 $R_{OL}$  = Outer zone left resistance reach  
 $R_{OR}$  = Outer zone right resistance reach

$LA$  = Line impedance angle  
 $X_{IT}$  = Inner zone top reactance reach  
 $X_{IB}$  = Inner zone bottom reactance reach  
 $X_{OT}$  = Inner zone top reactance reach  
 $X_{OB}$  = Inner zone top reactance reach

Figure 21: Out-of-step function (a) blinder scheme supervised with overcurrent function (b) quadrilateral scheme

## 10 Impact on Negative Sequence Functions

Synchronous machines inject a large amount of negative sequence current during unbalanced faults. This has traditionally been used for a number of protection functions in distance and overcurrent relays.

Inverter based generation typically is controlled to suppress negative sequence current contribution during a fault. As conventional generation is retired the lack of negative sequence contributions might cause significant mal-operation of relays across the network.

In distance relays some functions of interest which are likely to be affected are:

- Some algorithm specific impedance estimation
- Directional blocking
- Fault type identification

While this is a known potential issue no such issues were discovered in the lines studied. Mutual coupling was not included in the lines studied which may contribute to issues related to negative sequence functionality. This can be further investigated in subsequent works.

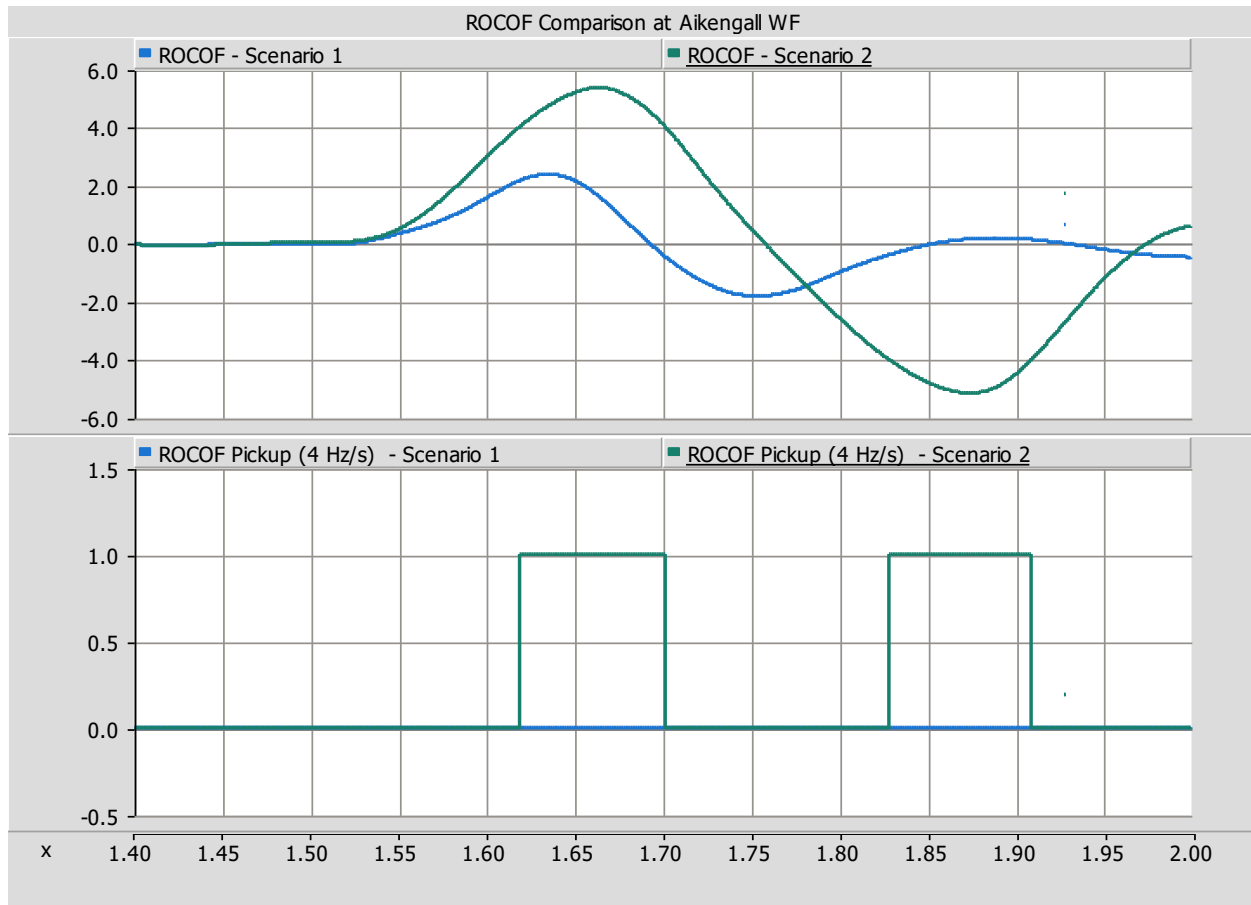
## 11 Impact on Rate-Of-Change-Of-Frequency and Vector Shift Relays

### 11.1 Rate-Of-Change-Of-Frequency (ROCOF) Relay

Reduction of system inertia causes a faster frequency deviation post fault or during loss-of-load / loss-of-generation. This is especially evident in areas of the network with very low levels of inertia. Local measurement of ROCOF may significantly differ from the national perceived levels. Rate-Of-Change-Of-Frequency relays ensure that specific elements disconnect during the large frequency deviations that typically occur when a portion of the network becomes islanded (disconnected from the main network).

Distributed generation typically contain a ROCOF setting in their connection relays. If ROCOF increases, the likelihood of significant loss of distributed generation during an existing frequency deviation will also increase. This can exacerbate the system condition. This occurred during the August 2019 outage and contributed to a historically low frequency deviation. Distributed generation is not typically monitored at a system operator level and as such it can be difficult to accurately determine the amount of low voltage distributed generation in service. This can be significant risk to system security.

While distributed generation was not included in this study model, as an example, a ROCOF relay was placed at Crystal Rig WF during two fault scenarios. The ROCOF significantly increased as shown in Figure 22 as the Torness generators were placed out of service and could be sufficient enough to cause a trip at the Point-of-Connection (POC) depending on the applied POC settings. This is an illustrative scenario though and may not represent the measurement ideology and filtering employed practically.



Scenario 1 - System normal, all power plants in service

Scenario 2 - N-1 one Branxton to Eccles line out, Torness 1/2 out-of-service, all other WF out-of-service

*Figure 22: ROCOF Comparison at Aikengall WF*

Some added frequency support may be required to mitigate frequency issues in the future. Fast frequency support controls on inverter based generation or synchronous condensers are likely solutions.

Additionally, as inertia providing sources are disconnected, the POC protection settings for all nearby plants should be investigated including ROCOF, over-frequency, and under-frequency.

## 11.2 Vector Shift (VSR) Relay

The vector shift relay is another method used to detect an islanding condition at the DG (also called Loss of Mains). A traditional VSR algorithm does this by comparing the angle difference between each successive positive and negative half cycles on each phase. Consider a single phase voltage measurement during a disturbance as shown in Figure 23.

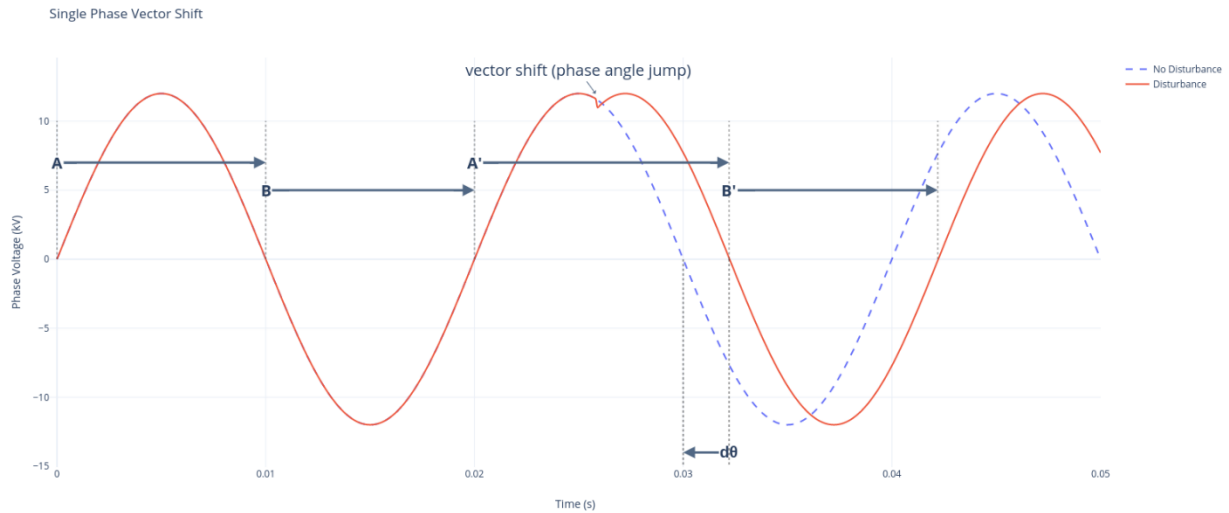


*Figure 23: Single phase vector shift during disturbance*

As each half cycle is completed (a zero crossing is encountered) its period is compared with the previous period of the same direction of half cycle (i.e. A' is compared with A, B' is compared with B). If the difference between periods is greater than the threshold (when converted to degrees based on nominal frequency) then a pickup occurs. For a single phase we have two comparisons (positive half cycle, negative half cycle) therefore when using all three phases there are six comparisons made. A final trip will only be issued if five out of six comparisons issue a pickup.

Since distributed generation was not included in this study model, as an example, a Vector Shift Relay was placed at Aikengall and Aikengall II wind farms for several scenarios and a greater than 15 degree phase angle jump was observed in all cases. This functionality is typically only included in small distributed generation.

Due to a high risk of disconnection Vector Shift Relays can no longer be used in the National Grid and must be upgraded to Rate-of-Change-of-Frequency (ROCOF) relays with an increased minimum disconnection setting of 1 Hz/s with a discrete time delay of 500 ms (previously 0.125 Hz/s).

## 12 Conclusion

Protection algorithms rely on the established characteristics of a typical grid (i.e. presence of synchronous machines). The increased penetration of inverter-based generation as well as the reduction in traditional synchronous machine sources will have a significant impact on a variety of protection systems. Assumptions used to make protection decisions in the past may no longer be valid. Additionally, simulation methods used to determine appropriate protection settings for each relay may no longer contain sufficient detail to capture all of the phenomenon associated with inverter-based technologies. The following protection relays and elements were identified as susceptible to mal-operation due to reduction in the fault current and inertia in the system.

Distance relay – The level of in-fault impedance point oscillation increases as system strength decreases. This can cause temporary zone 1 over-reach conditions. This was observed in simulation. This mal-operation was eliminated by substituting with a generic differential protection scheme.

Power Swing (Out-of-Step) Protection – Decreased system strength increases the likelihood of an unstable power angle swing across a protected transmission line. No out-of-step conditions were observed in simulation.

Negative sequence functions – Various functions in protection schemes rely on negative sequence measurements to make logic decisions. Examples include some impedance estimates, fault direction detection, and fault type identification. Low negative sequence current injection by nearby sources for unbalanced faults can prevent correct operation of these supervisory functions. This was not observed in simulation.

Rate-of-Change-of-Frequency (ROCOF) – Typical grid codes stipulate a level of ROCOF that sources are required to ride-through before disconnecting. Decreasing system inertia will potentially cause ROCOF protection trips, which can further exacerbate post disturbance conditions. A 200% increase in ROCOF was measured at Crystal Rig wind farm for a disconnection of Torness Power Plant and N-2 condition.

Any protection system changes will require a wide variety of non-traditional protection studies on a case-by-case basis to ensure proper operation occurs now and in the future.

As the vulnerability of protections to non-classical fault behaviour emerge, it is important that modelling both reflects the classical principle of relay operation and setting together with the vendor specific algorithms used to determine action and place relay measurement in context to the event being measured as both can be vulnerable to the less predictable and more dynamic fault current supplied by converter based sources within the network. Further work is required to improve models to capture vendor specific solutions in sufficient detail to enable realistic conclusions of actual relay behavior to be made.

## 13 Next Steps

While the level of detail presented in this report is sufficient to show some potential issues in general, it is not able to reliably pinpoint protection deficiencies at specific pieces of equipment in the network. The general models used do not represent the actual equipment well enough (especially with respect to control functions) to make policy decisions.

Further studies must be undertaken with an increased level of detail. The following steps for future studies can act as a starting point:

- 1) Update model in PSCAD™ to include detailed manufacturer models (including all control/protection loops) for all relevant equipment. Effect of saturation on current and voltage measurements can also be included with more detailed electromagnetic models of the measurement devices.
- 2) Using the improved PSCAD™ model from step one simulate instantaneous fault currents and voltages at the point of measurement for each of the surrounding protection relays using the Comtrade Recorder component present in PSCAD™. Import the recorded signals directly to the physical relay in question and simulate the response using the built in playback functionality.
- 3) Create a Hardwire-in-the-Loop (HIL) model of the same network area (Using software such as RSCAD®) and directly connect a physical relay to the HIL interface.

Additional forms of protection can also be added in each of these steps such as Bus, Transformer, and Generator protection relays. Adding more protection details will help mimic the potential loss of generation that can occur during fault disturbances.

## 14 References

[1] "National Trends and Insights (A System Operability Framework Document)", National Grid ESO,  
<https://www.nationalgrideso.com/document/190151/download>

[2] J. Holbach, R. Zhang, T. Charton, D. Kerven and S. Ward, "Protection functionality and performance with declining system fault levels and inertia within national grid electricity transmission system in the United Kingdom," 15th International Conference on Developments in Power System Protection (DPSP 2020), 2020, pp. 1-6, doi: 10.1049/cp.2020.0065.

[3] "Distance Relay Fundamentals", GE Power Management, GER-3966,  
<https://www.gegridsolutions.com/products/applications/ger3966.pdf>

[4] Xue, Y., Douglas I. Taylor and Yu Xia. "Line Differential Protection Under Unusual System Conditions." (2015). [https://cms-cdn.selinc.com/assets/Literature/Publications/Technical%20Papers/6568\\_LineDifferential\\_BK\\_20120904\\_Web.pdf?v=20201215-234228](https://cms-cdn.selinc.com/assets/Literature/Publications/Technical%20Papers/6568_LineDifferential_BK_20120904_Web.pdf?v=20201215-234228)